PROCEEDINGS OF SPIE

SPIEDigitalLibrary.org/conference-proceedings-of-spie

Influence of the fraction of absorbed pump power on the performance of Nd3+:YVO4 powder random lasers

Niklaus U. Wetter, Danilo A. A. da Silva, Ernesto Jimenez-Villar, Julia M. Giehl

Niklaus U. Wetter, Danilo A. A. da Silva, Ernesto Jimenez-Villar, Julia M. Giehl, "Influence of the fraction of absorbed pump power on the performance of Nd3+:YVO4 powder random lasers," Proc. SPIE 10528, Optical Components and Materials XV, 105281U (22 February 2018); doi: 10.1117/12.2290674

SPIE.

Event: SPIE OPTO, 2018, San Francisco, California, United States

Influence of the fraction of absorbed pump power on the performance of Nd^{3+}:YVO_4 powder random lasers

Niklaus U. Wetter*, Danilo A. A. da Silva, Ernesto Jimenez-Villar, Julia M. Giehl
Center for Lasers and Applications, Instituto de Pesquisas Energéticas e Nucleares IPEN-CNEN/SP,
Av. Prof. Lineu Preses, 2242, São Paulo, SP, Brazil

ABSTRACT

Understanding light absorption in random lasers and its distribution within the scattering gain media is a key issue to increase the lasers' efficiency. Here we compare monodispersed and polydispersed powders of Nd^{3+}:YVO_4 and investigate the influence of the powder size distribution on scattering mean free path, absorption volume and, eventually, the lasers efficiency. The highest efficiency is achieved for polydispersed powders and we conjecture that these polydispersed powders, composed of pockets containing small grains trapped between large particles, present locally higher pump power densities than the monodispersed powders. We establish a figure of merit, based on measurable powder parameters, that agrees well with the obtained output power results of the monodispersed and polydispersed samples.

Keywords: Random lasers, light scattering, neodymium lasers

1. INTRODUCTION

Random lasers were proposed for the first time in the 1960s by Lethokov[1,2] as being a means of generating stimulated emission using scattering media for radiation feedback instead of mirrors. The gain media itself can be the scattering media by using for example grind crystals or scattering media and gain media may be separated, as is the case with rutile (TiO_2) particles and a rhodamine solution, respectively. Random lasers can be easily and cost-effectively produced from many diverse materials such as ceramics, semiconductors[3], biological tissue and organic material in general[4], polymers[5], doped glasses and crystals[6]. Today, they are already used in applications such as speckle-free imaging in biology, remote-sensing, display technology, encrypting, cancer detection and distributed amplification[7].

Some characteristics of random lasers have hampered so far their use in a broader range of applications. These are mainly their lack of beam pointing capability and their low efficiency. Some specific types of random lasers may overcome these limitations such as 1-D and 2-D random lasers. For example, fiber-random lasers have demonstrated several watts of directional output power[8] and 2-D distributed feedback lasers have already demonstrated pulse formation in the micro joule range. However, these random lasers are bulky and require sophisticated production methods when compared to standard 3-D random lasers.

While we have treated the lack of beam directionality in a former publication of ours[9], the issue of low efficiency deserves special attention. M. A. Noginov et al. have studied the dependence of random laser emission in neodymium doped powders ($Nd_{0.5}La_{0.5}Al_3(BO_3)_4$) on the particle size, the powder volume density and the pump spot size.[10,11] Best reported efficiency was below half a percent. An impediment for increasing the efficiency is the surface reflectivity of the compacted powders. The bulk reflection coefficient of $Nd_{0.5}La_{0.5}Al_3(BO_3)_4$ at $\lambda = 532$ nm for medium to high powder density is approximately 0.7.[11] Using a fiber-coupled random laser, where the pump fiber terminates deep inside the scattering medium in order to deliver the pump energy directly into the gain volume without reflection loss at the surface, Noginov et al. achieved a higher efficiency of approximately 0.7 %.[12]

*nuwetter@ipen.br; phone =55 11 3133 9359; www.ipen.br

Optical Components and Materials XV, edited by Shibin Jiang, Michel J. F. Digonnet, Proc. of SPIE Vol. 10528, 105281U

Azkargorta et al. achieved 20% and 42% slope efficiencies with respect to pump power using Nd:YAG and $Nd_3Ga_5O_{12}$ crystal powders.[13,14] The jump in efficiency is due to way this output power was calculated. Taking into account that the emission from a powder pellet in the back direction goes into a solid angle of 2π and has the form of a Lambertian emission, they collected only the center part of a small solid angle and then calculated the whole emission.

Besides using random laser gain media that have shown exceptional efficiency when used as bulk lasers[15], other parameters can be optimized such as grain size and filling fraction. So far no attempt has been made, to our knowledge, to analyze the influence of polydispersed powders on the random laser efficiency. Here we propose a system containing different grain sizes using a high volume fraction of large grain sizes and small volume fraction of much smaller grain sizes. Although the volume occupied by the smaller grains is much smaller than the one occupied by the bigger particles, the absolute number of these smaller particles would be much bigger.

The immediate advantages of this strategy would be that there are pockets of smaller particles trapped between the larger particles with much smaller transport mean free path and, therefore, a higher density of absorbed pump power. This would cause a higher gain in these regions. Additionally, given the lower transport mean free path when compared to the average mean free path, these pockets would receive pump radiation not only from the pump facet, but also, given the longer transport mean free path of the larger particles, from all other sides. Whilest the smaller particles are responsible for much of the gain properties of the samples, the larger particles are responsible for the diffusion properties and determine the volume of the pumping region.

By comparing monodispersed with polydispersed samples, we demonstrate the validity of the above hypothesis, demonstrating comparable photon path length in both types of samples but considerably higher amount of scattering events in the polydispersed samples. Using this information, we create a figure of merit that agrees well with the output power results.

2. SAMPLE PREPARATION

Part of a Nd3+:YVO4 crystal containing 1.33 mol% neodymium doping was grinded to a powder. The powder was sieved using different mesh grids to obtain several ranges of particle sizes (see table 1). About 60 milligrams of powder were used to make a single pellet of 7 mm diameter. Different pressures were used to compact the pellets (shown in Table 1) however, here we only report on the pellets pressed with 250 MPa that gave the highest slope efficiency. Three pellets were produced per grain size and applied pressure. In order to determine the average particle size for each sieving range, the laser diffraction technique was used (CILAS model 106).

Table 1. Particle sizes and applied pressures of the Nd^{3+}(1.33 mol%):YVO4 powder pellets for the polydispersed groups A1 to A5.

Particle size	Group	Mean particle size	Applied pressure
$10 \leq x \leq 20$ μm	A1	10 μm	250 MPa
$20 \leq x \leq 45$ μm	A2	15 μm	250 MPa
$45 \leq x \leq 75$ μm	A3	30 μm	250 MPa
$75 \leq x \leq 106$ μm	A4	54 μm	250 MPa
$106 \leq x \leq 180$ μm	A5	230 μm	250 MPa

Scanning electron microscopy (SEM) images of the pellets were obtained, as for example, the sample of grain sizes in the range $10 \leq x \leq 20$ μm (pressed with 500 MPa), shown in Figure 1.

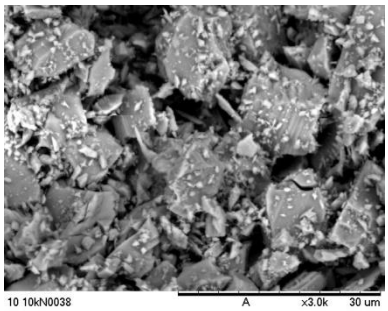

Figure 1: SEM image of powder sample from group A1 with particle size of in between 10 μm and 20 μm.

The particles presented irregular shape and the standard deviation of the size was on average close to the particle size itself, except for the very large particles. The groups A1 to A5 represent the polydispersed samples.

A second group, B1 to B5, received an additional cleansing procedure with the objective to get better monodispersed powders. This last procedure consisted of mixing isopropyl alcohol with the powders, stirring the liquid mechanically for 5 minutes in ultrasound, then sieving the mixture again and drying for a period of 24 hours. The result was satisfactory for the larger grain sizes, however, for a mesh size of 20 μm or less the procedure did not work properly and the powder still consisted of a mixture of large and small particles, as shown in Figure 2.

Table 2. Particle sizes and applied pressures of the Nd^{3+}(1.33 mol%):YVO4 powder pellets for the monodispersed groups B1 to B5.

Particle size	Group	Mean particle size
$10 \leq x \leq 20$ μm	B1	9.9 μm
$20 \leq x \leq 45$ μm	B2	37 μm
$45 \leq x \leq 75$ μm	B3	55 μm
$75 \leq x \leq 106$ μm	B4	96 μm
$106 \leq x \leq 180$ μm	B5	147 μm

Shown below is a typical sample of the B groups (group B2):

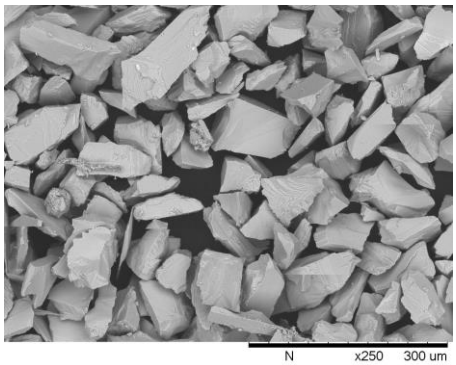

Figure 2: SEM image of powder sample from group B2.

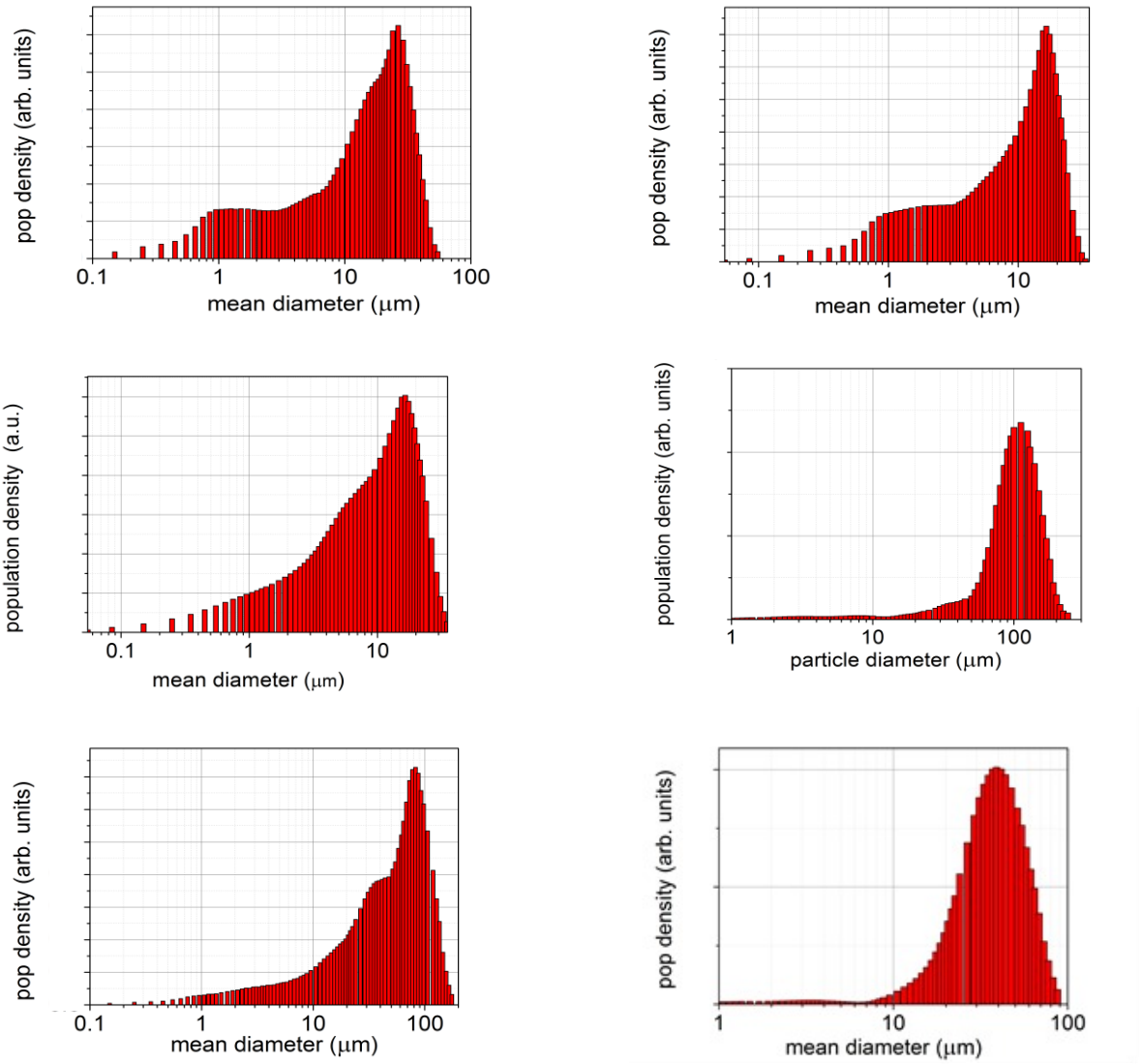

Figure 3: histograms of population density in volume from mixed samples of group A (left column) and cleansed samples B (right column). The images in the first row are from samples of group 1 (B1 and A1, respectively), the second row contains images from B2 and A2, respectively, and the last row B4 and A4. Histograms are not in scale.

3. EMISSION MEASUREMENTS

The laser set-up included a quasi-continuous (qcw), fast-axis-collimated laser diode bar with 150 μs pulse duration, operating at 806.5 nm with 5 Hz repetition rate. The laser beam was focused by an f = 20 mm spherical lens onto the powder pellets. A dichroic beamspitter separated the pump radiation from the neodymium laser emission at 1064 nm, which was collected either by a fiber for spectroscopic analysis or by a pyroelectric power meter for input-output power measurements. Maximum pump energy was 8.2 mJ. The sample was rotated at approximately 20 Hz.

A typical emission spectrum captured with the fiber-coupled spectrometer is shown in Figure 4. Clearly seen are the random laser emission peak at 1064 nm, a residual pump reflection at 806 nm and the fluorescence emission peaks of the $^4F_{3/2} \rightarrow {}^4I_{9/2}$ three-level transition around 900 nm. The insets demonstrate also that close to threshold there are no additional spikes or peaks beyond the fluorescent spectra and the central ASE peak.

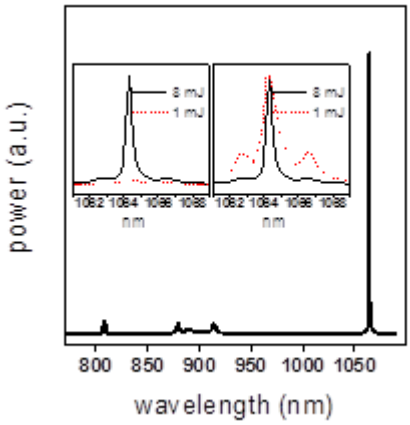

Figure 4: Measured emission spectra at maximum pump power (8 mJ) for a sample A_4. Insets: Emission of sample at 1064 nm for 8 mJ (solid lines) and 1 mJ (dotted lines) of pump power showing amplitudes in scale (left inset) and normalized amplitudes (right inset).

The maximum output pulse energy that was achieved as a function of each group is demonstrated in Table 3.

Table 3. Maximum output pulse energy achieved at 1064 nm using 150 μs pump pulse duration and 8.2 mJ at 808 nm.

Particle size	Group	Output pulse (mJ)	Group	Output pulse (mJ)
$10 \leq x \leq 20$ μm	A1	0.16	B1	0.11
$20 \leq x \leq 45$ μm	A2	0.36	B2	0.27
$45 \leq x \leq 75$ μm	A3	0.42	B3	0.58
$75 \leq x \leq 106$ μm	A4	1.3	B4	0.44
$106 \leq x \leq 180$ μm	A5	0.96	B5	0.33

As can be seen from above table, the highest efficiency is achieved for the polydispersed group A4. The optical efficiency in terms of absorbed pump power is 34% with a corresponding slope efficiency of 50%, which is the highest slope efficiency for random lasers reported so far, to the best of our knowledge, and that is comparable to diode pumped bulk-Nd:YVO_4 lasers! Its samples are 2.2 times more efficient than the best monodispersed samples (B3) and three times more efficient than the equivalent monodispersed samples (B4).

4. CALCULATION OF TRANSPORT MEAN FREE PATH AND FILLING FRACTION

A MATLAB program was used to calculate transport mean for path L_T for each group as a function of the population densities in volume obtained with the Fraunhofer diffraction technique. Because this technique uses a solution of particles, L_T is calculated for a filling fraction (*ff*) of one. An additional common backscattering cone (BSC) measuring set-up was used to measure L_T of the final pressed pellets. The ratio of the calculated L_T divided by the measured L_T gives the filling fraction *ff*. Detailed information on this measurements can be found elsewhere.[16]

It should be mentioned that for the samples composed of smaller grains, such as A1, A2 and B1, the smallest particles agglomerate, generating longer mean free path within the pellets. Notice that, as voids become more and more filled up, the smaller particles overcome the repulsive Coulomb forces and start to touch each other[17,18], building agglomerates[19,20,21]. For interparticle distances less than one wavelength, the agglomerate behave as a bigger particle with a lower effective refractive index and scattering cross-sections. These effects together, smaller effective scattering cross-section, smaller effective refractive index and several particles together, behaving like a single large particle (agglomerate), work in the direction of increasing L_T.

Therefore, another method had to be used to find the correct fill fraction for these groups. In our specific case we noted that the average spectrally integrated output power for very low pump powers is constant to within 5% for all groups. Therefore, at low pump powers, the ratio of the output powers of two different groups depends only on *ff* and L_T, allowing to calculate the missing filling fractions.

The filling fractions varied from 0.96 down to 0.59 for A1 to A5 and from 0.91 down to 0.57 for groups B1 to B5, whereas the transport mean free path varied from 2.3 to 4.9 and 2.4 to 5.2, respectively.

5. ABSORPTION AND REFLECTIVITY MEASUREMENTS

Low pump power absorption measurements were carried out at pump wavelengths (Agilent, model Cary 5000) of 705 nm (no absorption, only reflection) and 805 nm (absorption peak) using a integrating sphere. We designated the ratio between the pumping intensities reflected by the samples at 705 nm and 805 nm as the fraction of absorbed pumping (FAP) [22,23]. From natural logarithm of FAP, we can estimate the average photon path length (l_c) inside the sample before being reflected (equation 1) [24,25].

$$FAP = \frac{I_{R(705nm)}}{I_{R(805nm)}} \Rightarrow \ln(FAP) \approx {}^{l_c}/_{l_a} \rightarrow l_c \approx l_a \times \ln(FAP) \quad (1)$$

where l_a is the microscopic absorption length, which is the ballistic absorption length of 256 μm divided by *ff*.

In order to ascertain that FAP does not change as a function of pump power, we used a similar setup as described in item 3 with the addition of a second spectrometer (see Figure 5). To maintain the detection geometry constant, the laser diode power was set to the maximum and neutral density filters were used to vary the pumping power. The results demonstrated clearly that, different from other gain media [22,23,**Erro! Indicador não definido.**], there is no FAP decrease for pumping power around the random laser threshold. This is due to our gain medium (Nd^{3+}) being a four-level system and only a small percent of Nd^{3+} ions participate in the laser action.

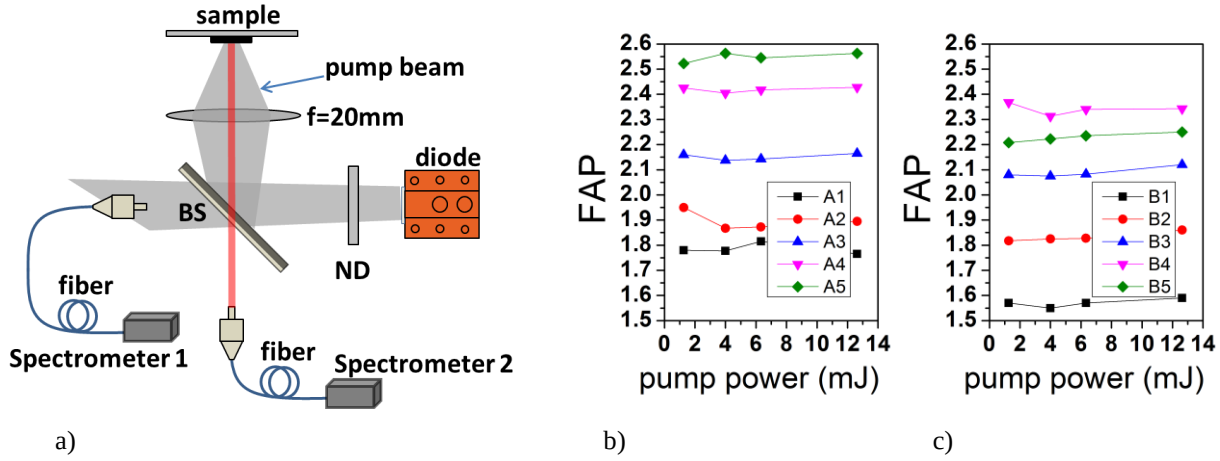

a) b) c)

Figure 5: Set-up used to measure FAP composed of the diode laser emitting at 805 nm, a beamsplitter (BS), an f=20 mm focusing lens and the sample mounted on a rotation stage. The pump power was varied using neutral density filters ND.The ratio of the two signals measured with the two fiber coupled spectrometers at 805 nm gives the fraction of absorbed pump power (FAP) shown in b) for the polydispersed and c) monodispersed groups as a function of pump power.

From the FAP measurements we calculate the resultant mean photon path length that range from 154 μm to 406 μm for groups A1 to A5 and from 127 μm to 360 μm for groups B1 to B5.

6. DISCUSSION

The quite similar results of FAP measurements for the polydispersed and monodispersed groups show clearly that the principal responsible for the macroscopic distribution of light within the samples are the bigger particles that are common to both groups.

It also can be observed from the FAP results that the A groups have slightly longer mean photon path length. If we take into account that the L_T values are smaller for the A groups and observe that l_c/ L_T is the number of scattering events that the backscattered pump photons undergo within the samples we calculate on average a 15% increase in scattering events for the polydispersed groups. This increase must be due to the additional smaller particles trapped in the pockets between larger particles in the case of the A groups. If we further take into account that the polydispersed groups have on average a 2% higher filling fraction, attributed to the additional pockets, we may correlate the 15% more absorbed energy to the 2% higher filling fraction resulting in a five times higher pump energy density within these pockets [16].

In order to establish a figure of merit we calculate the absorbed pump power, given by l_C*ff/l_a, and multiply the result by the pump energy density factor, l_c/ L_T, established above. The results are shown in Figure 6 and compare well with Table 3. For example, B3 and A4 are the best performing samples of the monodispersed and polydispersed groups, respectively, or, A3, B3 and B4 are of similar value.

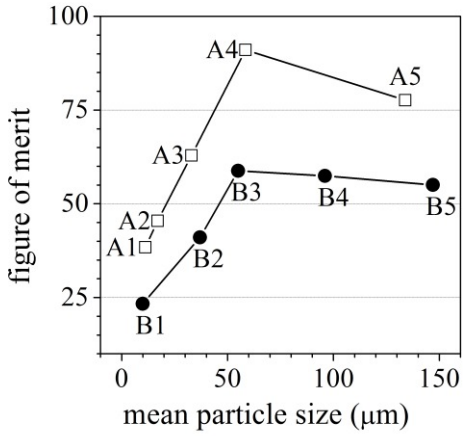

Figure 6: Figure of merit as a function of mean particle size for the different groups as define in the text.

7. CONCLUSIONS

Using a new strategy that used polydispersed powders to separate gain and pump light diffusion, we achieved, to our knowledge, the highest reported efficiency for 3-D random lasers. This increase of the random laser efficiency has been attributed to a notable increase of the photon path length and a slight decrease in transport mean free path, observed for the polydispersed size powders.

REFERENCES

[1] Letokhov, V. S., "Stimulated emission of an ensemble of scattering particles with negative absorption," JETP Lett. 5, 212-215 (1967).
[2] Letokhov, V. S., "Generation of light by a scattering medium with negative resonance absorption," Sov. Phys. JETP 26, 835-840 (1968).

[3] Cao, H., Zhao, Y. G., Ho, S. T., Seelig, E. W., Wang, Q. H. and Chang, R. P. H., "Random Laser Action in Semiconductor Powder," Phys. Rev. Lett. 82, 2278-2281 (1999).
[4] Polson, R. C., Vardenya, Z. V., "Random lasing in human tissues." Appl. Phys. Lett. 85, 1289–1291 (2004).
[5] Polson, R. C., Chipouline, A., Vardeny, Z. V., "Random Lasing in π-Conjugated Films and Infiltrated Opals," Adv. Mater. 13, 760–764 (2001).
[6] Wiersma, D. S., "The physics and applications of random lasers," Nat. Phys. 4, 359-367 (2008).
[7] Redding, B., Choma, M. A., Cao, H., "Speckle-free laser imaging using random laser illumination," Nat. Photonics 6, 355-359 (2012).
[8] Wang, Z., Wu, H., Fan, M., Zhang, L., Rao, Y., Zhang, W., Jia, X., "High Power Random Fiber Laser with Short Cavity Length: Theoretical and Experimental Investigations," IEEE J. Sel. Top. Quantum Electron. 21, 0900506 -900511, (2015).
[9] Jorge, K. C., Alvarado, M. A., Melo, E. G., Carreño, M. N. P., Alayo, M. I., Wetter, N. U., "Directional random laser source consisting of a HC-ARROW reservoir connected to channels for spectroscopic analysis in microfluidic devices," Appl. Opt. 55, 5393-5398 (2016).
[10] Bahoura, M., Morris, K. J., Zhu, G. and Noginov, M. A., "Dependence of the neodymium random laser threshold on the diameter of the pumped spot," IEEE J. Quantum Electron. 41(5), 677-685 (2005).
[11] Noginov, M. A., Noginova, N. E., Egarievwe, S. U., Caulfield, H. J., Cochrane, C., Wang, J. C., Kokta, M. R., Paitz, J., "Study of the pumping regimes in Ti-sapphire and Nd0.5La0.5Al3(BO3)4 powders," Opt. Mat. 10, 297-303 (1998).
[12] Noginov, M. A., Fowlkes, I. N., and Zhu, G., "Fiber-coupled random laser," Appl. Phys.Lett. 86, 161105/1-5 (2005).
[13] Azkargorta, J., Iparraguirre, I., Barredo-Zuriarrain, M., García-Revilla, S., Balda, R., Fernández, J., "Random Laser Action in Nd:YAG Crystal Powder," Materials 9, 369 (2016).
[14] Iparraguirre, I., Azkargorta, J., Kamada, K., Yoshikawa, A., Rodríguez-Mendoza, U.R., Lavín, V., Barredo-Zuriarrain, M., Balda, R., Fernández, J., "Random laser action in stoichiometric $Nd_3Ga_5O_{12}$ garnet crystal powder," Laser Phys. Lett., 13, 035402-035405 (2016).
[15] Vieira, R. J. R., Gomes, L., Martinelli, J. R. and Wetter, N. U.,"Upconversion luminescence and decay kinetics in a diode-pumped nanocrystalline Nd3+:YVO4random laser," Opt. Express **20**, 12487-12497 (2012).
[16] Wetter, N. U., Giehl, J. M., Butzbach, F., Anacleto, D., Jiménez-Villar, E., "Polydispersed Powders (Nd^{3+}:YVO_4) for Ultra Efficient Random Lasers," Part. Part. Syst. Charact. 2017, 1700335-1700345 (2017).
[17] Jimenez, E., et al. "A novel method of nanocrystal fabrication based on laser ablation in liquid environment," Superlattices and Microstructures **43**, 487–493 (2008).
[18] Gonzalez-Castillo J. R., et al. "Synthesis of Ag@Silica Nanoparticles by Assisted Laser Ablation," Nanoscale Research Letters **10**(1), p9 (2015).
[19] Fuertes, G., et al. "Switchable bactericidal effects from novel silica-coated silver nanoparticles mediated by light irradiation," Langmuir **27**, 2826–2833 (2011).
[20] Jimenez, E., Abderrafi, K., Abargues, R., Valdes, J. L., Martınez-Pastor, J. "Laser-ablation-induced synthesis of SiO2-capped noble metal nanoparticles in a single step," Langmuir **26**, 7458–7463 (2010**)**.
[21] Ermakov, V. A., Jimenez-Villar, E., Silva Filho, J. M. C. da, Yassitepe, E., Mogili, N. V. V., Iikawa, F., de Sá, G. F., Cesar, C. L. and Marques, F. C., "Size Control of Silver-Core/Silica-Shell Nanoparticles Fabricated by Laser-Ablation-Assisted Chemical Reduction," Langmuir **33**(9), 2257–2262 (2017)
[22] Jimenez-Villar, E., Mestre, V., Oliveira P. C. & de Sá, G. F. "Novel core–shell (TiO2@Silica) nanoparticles for scattering medium in a random laser: higher efficiency, lower laser threshold and lower photodegradation," Nanoscale **5**, 12512–12517 (2013).
[23] Jimenez-Villar, E., et al. "TiO2@Silica nanoparticles in a random laser: Strong relationship of silica shell thickness on scattering medium properties and random laser performance," Appl. Phys. Lett. **104**, 081909 (2014).
[24] Jimenez-Villar, E., et al. "Anderson localization of light in a colloidal suspension (TiO2@Silica)," Nanoscale**,** **8**(21), 10938–10946 (2016).
[25] Jiménez-Villar, E., Da Silva, I. F., Mestre, V., Wetter, N. U., Lopez, C., De Oliveira, P. C., Faustino, W. M. and De Sá, G. F., "Random lasing at localization transition in a colloidal suspension (TiO2@Silica)," ACS Omega **2**, 2415–2421 (2017).